Journal of Alloys and Compounds 648 (2015) 190–194

Contents lists available at ScienceDirect

Journal of Alloys and Compounds

journal homepage: http://www.elsevier.com/locate/jalcom

Urea-assisted hydrothermal synthesis of manganese dioxides with various morphologies for hybrid supercapacitors

Ling Kang, Lining Zhang, Huijun Zou, Zhongxu Deng, Yue Zhang, Lianmei Chen*

Chemical Synthesis and Pollution Control Key Laboratory of Sichuan Province, College of Chemistry and Chemical Engineering, China West Normal University, Nanchong, Sichuan 637000, China

ARTICLE INFO

Article history:
Received 8 May 2015
Received in revised form
25 June 2015
Accepted 26 June 2015
Available online 30 June 2015

Keywords:
MnO_2
Thorn spheres
Long nanowires
Hybrid supercapacitors
Li_2SO_4 electrolyte

ABSTRACT

Two MnO_2 samples (MO-1 with thorn spheres and MO-2 with long nanowires) were synthesized by adding urea into $KMnO_4$–H_2SO_4 reaction system at various hydrothermal temperatures. Urea could decrease the reaction temperature, and its hydrolysis could influence the morphology of MnO_2. The as-prepared samples were analyzed by XRD and SEM. Their capacitive properties were investigated by electrochemical impedance spectroscopy, cyclic voltammetry and galvanostatic charge/discharge test. The initial specific capacitance values of AC//MO-1 and AC//MO-2 hybrid capacitors were 24.99 and 27.58 F g^{-1} in 1 M Li_2SO_4 electrolyte, respectively. After 1000 cycles, the capacitance retention was 91.40% for AC//MO-1 and 96.93% for AC//MO-2. Therefore, AC//MO-2 exhibited better capacitive properties than AC//MO-1.

1. Introduction

Supercapacitors are becoming attractive energy store devices due to their potential applications in hybrid electric vehicles, burst power generation, memory back-up devices, and so on [1–3]. On the basis of the charge storage mechanism as well as the active materials used, there are two major categories: electric double-layer capacitors (EDLCs) and pseudo-capacitors. EDLCs employ various kinds of nanoporous carbons, which rapidly charge/discharge but display relatively low capacitance [4–6]. Pseudo-capacitors utilize transition metal oxides or conducting polymers [7–18], which often provide high capacitance but deliver low power density or suffer from instability during cycling process. In order to deliver high specific capacitance in combination with high power density, considerable efforts have been devoted to various hybrid supercapacitors in which transition metal oxides or conducting polymers was used as positive materials (energy source), and activated carbon (AC) was used as negative material (power source), such as AC//MnO_2 [19–25], AC//$Ni(OH)_2$ [26–28], AC//V_2O_5 [29], AC//PPy [30], AC//PAn [31], etc. The hybrid cells can extend the work voltage beyond the thermodynamic limit (about 1.2 V) in aqueous electrolyte, contributing to significant improvement in the specific energy. AC//MnO_2 supercapacitor is a representative of these hybrid systems due to good performance, abundant resources, low cost and environmental friendliness.

Electrochemical properties of MnO_2 strongly depend on the crystal structure, dimension, morphology, and thickness because these factors would influence the electronic conductivity and the penetration of electrolyte ions [32,33]. Cheng et al. [34] prepared α-MnO_2 nanospheres/nanosheets in $KMnO_4$–H_2SO_4 reaction system at 160 °C for 10 h. Yin et al. [35] successfully synthesized different MnO_2 structures by controlling the concentration of K^+ and H^+ in $KMnO_4$–HNO_3 reaction system at 160 °C for 24 h. The results indicated that β-MnO_2 particles were obtained when H^+ ions was more than K^+ ions; and α-MnO_2 nanorods were formed when K^+ ions was more than H^+ ions. In our work, urea, as a weak reducing agent, was added into $KMnO_4$–H_2SO_4 reaction system to decrease the reaction temperature. Meanwhile, the hydrolysis of urea could change the concentration of H^+ [36], and consequently influence the morphology of α-MnO_2. Therefore, the morphologies of α-MnO_2 samples in our work were different from the nanospheres/nanosheets or nanorods reported in the references [34,35].

Under the urea-assisted hydrothermal condition, α-MnO_2 thorn spheres (MO-1) were synthesized at 100 °C for 8 h in $KMnO_4$–H_2SO_4 reaction system. However, when the reaction temperature increased to 180 °C, α-MnO_2 long nanowires (MO-2) were formed. Their capacitive properties were investigated in aqueous hybrid supercapacitors (AC//MnO_2). Li_2SO_4 solution was

* Corresponding author.
E-mail address: chenlm0817@163.com (L. Chen).

http://dx.doi.org/10.1016/j.jallcom.2015.06.230
0925-8388/

adopted as the electrolyte because the stronger hydration of Li^+ ions is responsible for larger working voltage and better cycling performance in comparison with Na^+ and K^+ [6]. The results showed that AC//MO-2 exhibited better capacitive properties than AC//MO-1, which was attributed to two factors: (i) the smaller resistance of MO-2 nanowires and (ii) the Faradaic reactions occurring on the surface and in the bulk of MO-2 nanowires.

2. Experimental

2.1. Preparation and characterization of manganese dioxide samples

In a typical process, 1.00 g of $KMnO_4$ was put into 35 ml of distilled water to form a homogeneous solution, and pH of the solution was adjusted to 0.5 using concentrated H_2SO_4. Afterward, 0.76 g of urea was added under magnetic stirring. The resultant transparent solution was transferred into a Teflon-lined autoclave with 50 ml, tightly sealed and kept at 100 or 180 °C for 8 h. After the reaction system was cooled to room temperature naturally, the brown-black precipitate was filtered and washed with deionized water and absolute ethanol thoroughly, and finally dried under vacuum condition (70 °C) for 24 h. For convenience, the samples prepared at 100 and 180 °C were labeled as MO-1 and MO-2, respectively.

The phase identity and crystal structure of the samples were examined by power X-ray diffractometer (XRD, Rigaku D/MAX-rA, Japan) equipped with Cu Kα radiation (λ = 0.15418 nm). Their morphology and size were characterized with scanning electron microscopy (SEM, JEOL JSM-6510LV, Japan).

2.2. Fabrication and electrochemical measurements of the MnO_2 and AC electrodes

The MnO_2 electrodes were fabricated by mixing 70 wt.% MnO_2, 25 wt.% acetylene black conductor, and 5 wt.% polyvinylidene fluoride (PVDF) binder in the *N*-methyl-2-pyrrolidine (NMP) solvent. The formed slurry was dried with infrared lamp to evaporate most of the NMP solvent. The resultant mixture powders were pressed onto round-shaped stainless steel grids (diameter 0.5 cm) and dried under vacuum condition (70 °C) to remove the residual solvent. The AC electrode was also prepared similarly. AC is provided by the Fuzhou Yihuan Carbon Co., Ltd (Fuzhou, China).

The electrochemical impedance spectroscopy (EIS) and cyclic voltammetry (CV) test were conducted by a CHI660E electrochemical workstation system in a three-electrode system with a MnO_2 electrode (or AC electrode), a platinum electrode and a saturated calomel electrode (SCE). The frequency range was typically set between 100 kHz and 0.01 Hz in EIS tests. The working voltage was set between 0 and 1.4 V in CV tests.

The charge/discharge test was performed in a two-electrode cell with MnO_2 positive electrode and AC negative electrode. A Teflon gasket (inner-diameter 5 mm, thickness 3 mm) was used as the separator between the two electrodes. The experiments were carried out by Neware battery program-control testing system.

All electrochemical tests were performed at room temperature in 1 M Li_2SO_4 solution.

3. Results and discussion

3.1. XRD analysis

Fig. 1 shows the XRD patterns of MO-1 and MO-2 samples. The two XRD profiles were similar, and all the peaks could be indexed to α-MnO_2 phase (JCPDS No. 44–0141) [37]. It was noteworthy that

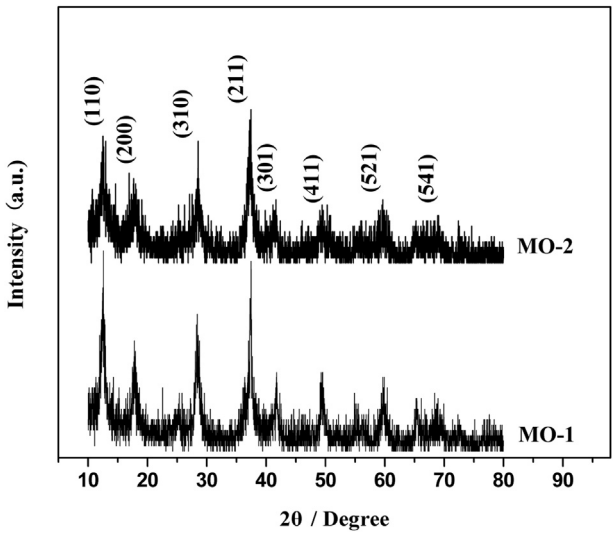

Fig. 1. XRD patterns of MO-1 and MO-2 samples.

the (110) peak was the strongest in the MO-1 pattern, but the (110) peak became weak and the (211) peak became the strongest in the MO-2 pattern. This result indicated that the preferred orientation growth of the individual α-MnO_2 structure was along the (211) facet at high hydrothermal temperature.

3.2. SEM analysis

The SEM images of MO-1 and MO-2 are presented in Fig. 2a and b. It is clear that MO-1 comprised micrometer-scale thorn spheres (Fig. 2a), whereas MO-2 mainly consisted of well-interconnected long nanowires (Fig. 2b). When the temperature increased from 100 to 180 °C, short and slim thorns inclined to grow along 1D direction and form long nanowires because of their energy differences. Meanwhile, larger amount of NH_3, which was released from the hydrolysis of urea, decreased rapidly the concentration of H^+ at 180 °C, so K^+ ions were much more than H^+ ions. Consequently, K^+ ions easily inserted into tunnels and stabilized the (2 × 2) tunnel structure [35,37], which was favorable to form long nanowires.

3.3. Electrochemical analysis

3.3.1. Electrochemical impedance spectroscopy (EIS) measurement

Alternating current impedances of MO-1 and MO-2 electrodes were measured with a three-electrode system in 1 M Li_2SO_4 solution, and their impedance spectra were illustrated in Fig. 3. All curves consisted of a semicircle in the high frequency and a linear region in low frequency range. The charge transfer resistance could be estimated from the diameter of the semicircle. As shown in Fig. 3, the resistance of MO-2 was smaller than that of MO-1, revealing that the long nanowires could improve the charge transfer efficiency.

3.3.2. Cyclic voltammetry analysis

The cyclic voltammetry (CV) tests of MO-1 and MO-2 electrodes were also done with the three-electrode system in 1 M Li_2SO_4 solution. The CV curves recorded for MO-1 electrode exhibited approximately rectangular-shaped profile (Fig. 4), which was in agreement with the results reported in the most of references [10,12,22–25]. However, a pair of broad redox peak was obviously observed from the CV curves recorded for MO-2 (Fig. 5), which was rarely reported. The results suggested that MO-1 and MO-2 varied slightly in the charge storage mechanism.